



Contents lists available at SciVerse ScienceDirect

Tetrahedron Letters

journal homepage: [www.elsevier.com/locate/tetlet](http://www.elsevier.com/locate/tetlet)

## Two new self-assemblies of two zinc porphyrin with isonicotinic acid by metal–ligand axial coordination and their applications in supramolecular solar cell

Jing Cao<sup>a</sup>, Jia-Cheng Liu<sup>a,\*</sup>, Li-Wei Chen<sup>a</sup>, Ren-Zhi Li<sup>b</sup>, Neng-Zhi Jin<sup>c</sup>

<sup>a</sup>Key Laboratory of Eco-Environment-Related Polymer Materials of Ministry of Education, Key Laboratory of Polymer Materials of Gansu Province, Key Laboratory of Bioelectrochemistry & Environmental Analysis of Gansu Province, College of Chemistry and Chemical Engineering, Northwest Normal University, Lanzhou 730070, PR China

<sup>b</sup>State Key Laboratory of Polymer Physics and Chemistry, Changchun Institute of Applied Chemistry, Chinese Academy of Sciences, Changchun 130022, PR China

<sup>c</sup>Gansu Computing Center, Lanzhou 730030, PR China

### ARTICLE INFO

#### Article history:

Received 8 March 2013

Revised 25 April 2013

Accepted 10 May 2013

Available online xxxxx

#### Keywords:

Self-assembly  
Zinc porphyrin  
Solar cell

### ABSTRACT

Two new self-assemblies based on two zinc porphyrins substituted at the meso-positions with different donor units (denoted as **ZnP1** and **ZnP2**) and isonicotinic acid (**A**) by metal–ligand axial coordination have been designed and immobilized on the double-layer nanostructured TiO<sub>2</sub> film-coated highly transparent FTO conducting glass electrode in a photosynthesis device. These cells were also measured under irradiance of 100 mW cm<sup>-2</sup> AM 1.5G sunlight. The results reveal that the performance of **ZnP2-A** outperforms that of **ZnP1-A**. The UV–vis absorption spectra, fluorescence spectra, molecular orbital (MO) patterns, and HOMO–LUMO energy gaps of these assemblies were also investigated to further demonstrate the photovoltaic behavior of these cells.

© 2013 Elsevier Ltd. All rights reserved.

Inspired by the model of the chromophores of bacterial photosynthetic reaction centers, utilization of the multiporphyrin-based self-assemblies formed by non-covalent interaction (such as  $\pi$ – $\pi$  stacking and weak van der Waals interaction) as sensitizers to mimic the photoinduced energy and electron transfer processes in solar cells have attracted increasing interests recently.<sup>1–6</sup> For example, several groups have constructed zinc(II) porphyrin-based supramolecular assemblies by the coordination bonds of Zn-to-ligand to functionalize carbon nanotubes,<sup>7–9</sup> gold electrode,<sup>10,11</sup> and nanoparticles,<sup>12–15</sup> with an ultimate goal of generating efficient light-energy-harvesting devices employing these assemblies. However, to the best of our knowledge, the reports about the assembly architecture based on zinc porphyrin appended organic acid via metal–ligand axial coordination approach immobilized on nano-structured TiO<sub>2</sub> substrates are very few.<sup>16,17</sup>

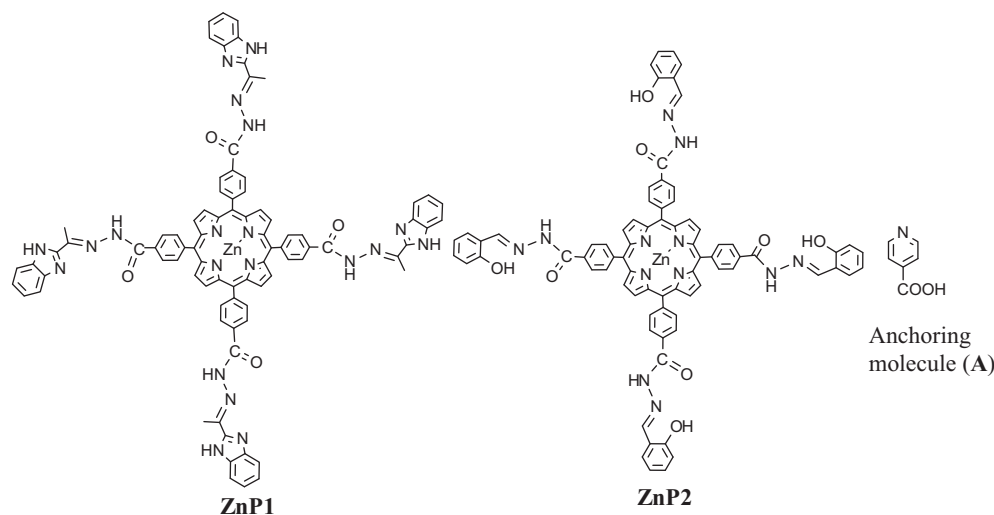
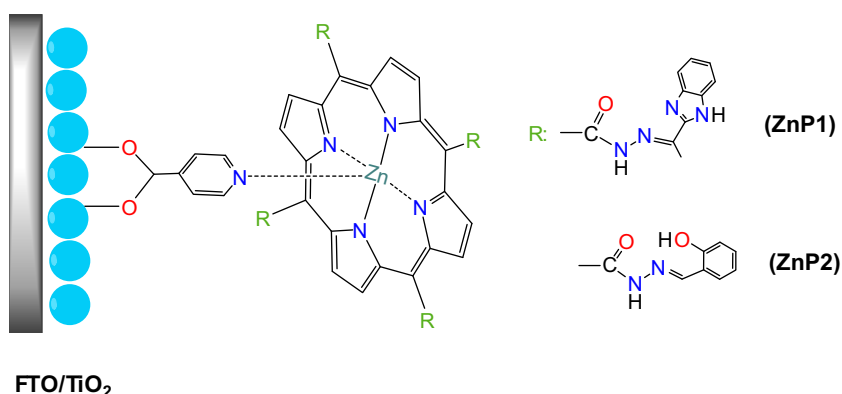
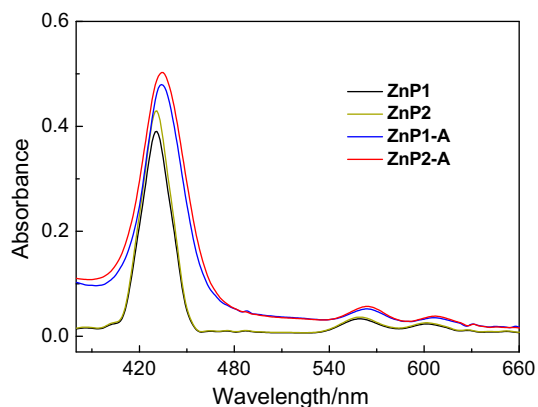
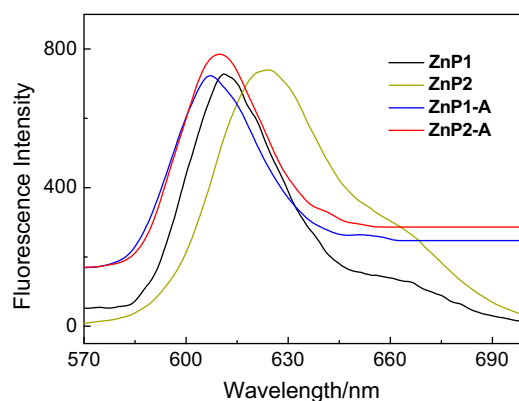
Herein, we report two new self-assemblies (described as **ZnP<sub>x</sub>-A**, **x** = 1, 2) with two zinc porphyrins substituted at the meso-positions with different units (denoted as **ZnP<sub>x</sub>**, **x** = 1, 2, shown in Scheme 1) and isonicotinic acid (denoted as **A**, shown in Scheme 1) by metal–ligand axial coordination, wherein these assemblies were immobilized directly on the double-layer nanostructured TiO<sub>2</sub> film-coated highly transparent FTO conducting glass electrode in a photosynthesis device. To probe into the impact of different do-

nor groups on the photoelectronic performance of their corresponding cells, two different donor units (phenol and benzimidazolyl) of these assemblies were introduced. The UV–vis absorption spectra, fluorescence spectra, molecular orbital (MO) patterns, HOMO–LUMO energy gaps, and the photovoltaic performance of these photosynthesis devices are also studied to further understand these assemblies-sensitized solar cells.

The synthetic steps are shown in [Supplementary data](#) and **ZnP<sub>x</sub>-A** are purple solids. The assembled processes of **ZnP<sub>x</sub>-A** on TiO<sub>2</sub> surface are as follows: **A** as anchoring unit was immobilized on the surface of the double-layer nanostructured TiO<sub>2</sub> film-coated highly transparent FTO conducting glass electrode<sup>18</sup> through carboxylic groups, then the desired dye of **ZnP<sub>x</sub>** was bound to the anchoring groups through coordination-bonded from porphyrin central Zn(II) ions of **ZnP<sub>x</sub>** and the N atoms of **A**. The detailed assembly mode is shown in [Scheme 2](#).

The parameters of UV–vis absorption and fluorescence spectra of **ZnP<sub>x</sub>** in solid state and **ZnP<sub>x</sub>-A** on TiO<sub>2</sub> thin film are summarized in Table S1. As shown in [Figure 1](#), these absorption maxima are displayed in the range of 400–480 nm for strong Soret (B) bands and 550–630 nm for Q bands, respectively, ascribed to  $\pi$ – $\pi^*$  transitions.<sup>19</sup> The absorption of **ZnP2-A** shows slight red-shift relative to that of **ZnP1-A**, which showed good agreement with the variation of HOMO–LUMO gaps, probably assigned to the donating ability of the phenol group over that of the benzimidazolyl unit. Interestingly, the absorption of **ZnP<sub>x</sub>-A** pronounces broadening and red-shifts compared with that of **ZnP<sub>x</sub>**. [Figure 2](#) compares

\* Corresponding author. Tel.: +86 9317971039; fax: +86 9317971989.  
E-mail address: [jliliu8@nwnu.edu.cn](mailto:jliliu8@nwnu.edu.cn) (J.-C. Liu).

Scheme 1. Structural diagram of **ZnP<sub>x</sub>** and anchoring molecule (**A**).Scheme 2. The detailed assembly approach of these assemblies on  $\text{TiO}_2$  electrode surface.Figure 1. UV-visible spectra of **ZnP<sub>x</sub>** in solid state and **ZnP<sub>x</sub>-A** on  $\text{TiO}_2$  thin film.Figure 2. Fluorescence spectra of **ZnP<sub>x</sub>** in solid state and **ZnP<sub>x</sub>-A** on  $\text{TiO}_2$  thin film.

the fluorescence spectra of **ZnP<sub>x</sub>** and **ZnP<sub>x</sub>-A**. The results reveal that the latter show blue-shift than the former, especially, the shift range between **ZnP1** and **ZnP1-A** is longer than that of **ZnP2** and **ZnP2-A**, suggesting that the presence of J-aggregation<sup>16</sup> of porphyrin assemblies for **ZnP<sub>x</sub>-A** devices on the  $\text{TiO}_2$  surface, and the aggregation of **ZnP1-A** show more than that of **ZnP2-A**.

In order to further understand the electron density distribution within the frontier and other neighboring orbitals of these assemblies, we performed calculations with density functional theory

(DFT) using the GAUSSIAN 09 program<sup>20</sup> at the B3LYP/LanL2DZ level. As shown in Figure S1, for **ZnP<sub>x</sub>-A**, the MO patterns of HOMOs are mainly localized at porphyrin cores with slight delocalization to the donor units, while the LUMOs show an electronic distribution on isonicotinic acid groups, signifying the presence of excellent electron-separated status for these assemblies-sensitized devices. Figure 3 shows the energy-levels diagram of these assemblies and  $\text{TiO}_2$ . The energy gap between the HOMO and LUMO is 2.22 eV for **ZnP1-A**, and 2.15 eV for **ZnP2-A**, to some extent

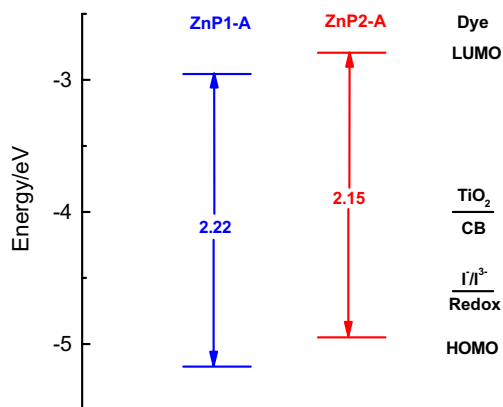


Figure 3. Orbital energy-levels of these assemblies, TiO<sub>2</sub>, and electrolyte I<sup>3-</sup>/I<sup>-</sup>.

indicating that the assembly of **ZnP2-A** should have a higher efficiency for corresponding device.<sup>21</sup> Notedly, the LUMO levels of these assemblies above that of the conducting band (CB) of TiO<sub>2</sub>, and the HOMO levels below that of the electrolyte I<sup>3-</sup>/I<sup>-</sup>, suggest that electron injection from LUMO of these assemblies to the CB of TiO<sub>2</sub> should be capable and feasible and the excited state of these assemblies could be reduced smoothly by the electrolyte.

The self-assemblies of **ZnP<sub>x</sub>-A** were fabricated into DSSC devices and tested their corresponding photovoltaic properties under irradiance of 100 mW cm<sup>-2</sup> AM 1.5G sunlight. The photovoltaic parameters are listed in Table 1. The photocurrent action spectra of **ZnP<sub>x</sub>-A**-sensitized solar cells in the wavelength range 300–800 nm shown in Figure 4 are analogous to their respective UV-vis spectra except for broader features, and consistent with the variation of HOMO–LUMO gaps, demonstrating the responsibility of photovoltaic behavior of these assemblies-sensitized solar cells. The maximum value of **ZnP2-A** device approaching 60% is significantly larger than that of the **ZnP1-A** device. As shown in Figure 5, the short-circuit photocurrent density (*J*<sub>sc</sub>), open-circuit photovoltage (*V*<sub>oc</sub>), fill factor (FF), and overall conversion efficient (*η*) are found to be 4.03 mA cm<sup>-2</sup>, 0.40 V, 0.70, and 1.12% for **ZnP1-A** device; 4.98 mA cm<sup>-2</sup>, 0.30 mV, 0.69, and 1.34% for **ZnP2-A** device. These results suggest that the phenol group increases the IPCE va-

Table 1  
Photovoltaic parameters of **ZnP1-A**/**ZnP2-A**-sensitized solar cells

Dye	<i>J</i> <sub>sc</sub> (mA cm <sup>-2</sup> )	<i>V</i> <sub>oc</sub> /V	FF	<i>η</i> (%)
<b>ZnP1-A</b>	4.03	0.40	0.70	1.12
<b>ZnP2-A</b>	4.98	0.30	0.69	1.34

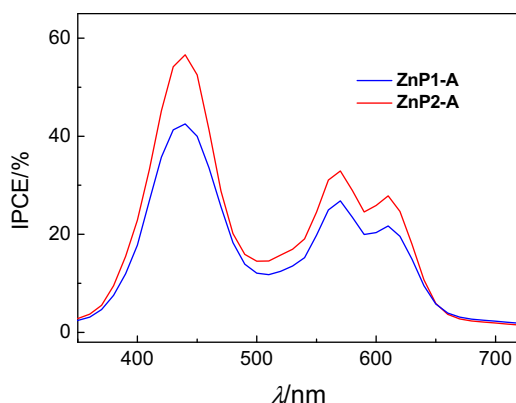


Figure 4. Photocurrent action spectra of **ZnP<sub>x</sub>-A**-sensitized solar cells.

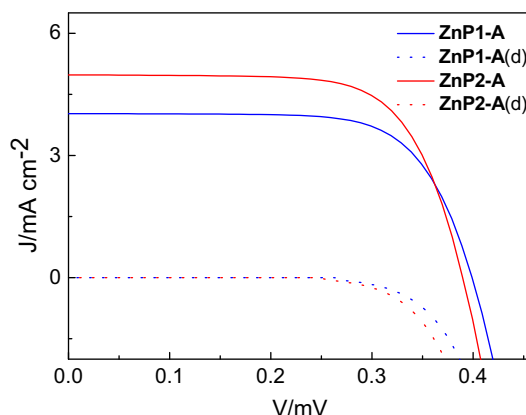


Figure 5. *J*–*V* characteristics of **ZnP<sub>x</sub>-A**-sensitized SC measured under irradiance of 100 mW cm<sup>-2</sup> AM 1.5G sunlight (**ZnP<sub>x</sub>-A**) and in the dark (**ZnP<sub>x</sub>-A(d)**).

lue of latter than the former to enhance the cell behavior of the latter. However, the larger *V*<sub>oc</sub> in **ZnP1-A** compared to **ZnP2-A** device is observed, probably assigned to the effect of aggregation.<sup>22</sup> Notedly, the poor efficiency of these assemblies may be assigned to the inefficient absorption of porphyrin molecules on red-NIR optical range.

In summary, we have successfully designed and obtained two new self-assemblies based on two zinc porphyrins **ZnP1** and **ZnP2** bound to isonicotinic acid by metal–ligand axial coordination. The UV–vis absorption spectra, fluorescence spectra, and the photovoltaic performance of these photosynthesis devices are also described. Our results reveal that these photosynthesis devices enable attainment of impressive improvement in photocurrent response, especially for **ZnP2-A** based on the substituent of phenol over the **ZnP1-A** substituted with benzimidazolyl. Additionally, the molecular orbital (MO) patterns and HOMO–LUMO energy gaps of these assemblies are also studied to further demonstrate these experimental products. Further study about the construction of similar assembly is on process.

## Acknowledgements

The National Natural Science Foundation of China (No. 20871099) and Gansu provincial Natural Science Foundation of China (No. 0710RJA113) have supported this work. We are very grateful to Professor Peng Wang (Changchun Institute of Applied Chemistry, Chinese Academy of Sciences) for supplying device fabrication and measurement of solar cell. We also thank the support of Gansu Computing Center of China.

## Supplementary data

Supplementary data associated with this article can be found, in the online version, at <http://dx.doi.org/10.1016/j.tetlet.2013.05.043>.

## References and notes

- D'Souza, F.; Amin, A. N.; El-Khouly, M. E.; Subbaiyan, N. K.; Zandler, M. E.; Fukuzumi, S. *J. Am. Chem. Soc.* **2012**, *134*, 654–664.
- Ichiki, T.; Matsuo, Y.; Nakamura, E. *Chem. Commun.* **2013**, 279–281.
- Zhou, H. X.; Yang, L. Q.; Stuart, A. C.; Price, S. C.; Liu, S. B.; You, W. *Angew. Chem., Int. Ed.* **2011**, *123*, 3051–3054.
- Krebs, F. C.; Tromholt, T.; Jørgensen, M. *Nanoscale* **2010**, *2*, 873–886.
- Yu, K. H.; Chen, J. H. *Nanoscale Res. Lett.* **2009**, *4*, 1–10.
- Yang, X. N.; Loos, J. *Macromolecules* **2007**, *40*, 1353–1362.
- Lee, J. M.; Park, J. S.; Lee, S. H.; Kim, H.; Yoo, S.; Kim, S. O. *Adv. Mater.* **2011**, *23*, 629–633.

8. Choi, H.; Kim, H.; Hwang, S.; Choi, W.; Jeon, M. *Sol. Energy Mater. Sol. Cells* **2011**, *95*, 323–325.
9. Li, G. R.; Wang, F.; Jiang, Q. W.; Gao, X. P.; Shen, P. W. *Angew. Chem., Int. Ed.* **2010**, *49*, 3653–3656.
10. Lai, W. H.; Su, Y. H.; Teoh, L. G.; Hon, M. H. *J. Photochem. Photobiol., A* **2008**, *195*, 307–313.
11. Wang, D. H.; Kim, D. Y.; Choi, K. W.; Seo, J. H.; Im, S. H.; Park, J. H.; Park, O. O.; Heeger, A. J. *Angew. Chem., Int. Ed.* **2011**, *123*, 5633–5637.
12. Kwak, E. S.; Lee, W.; Park, N. G.; Kim, J.; Lee, H. *Adv. Funct. Mater.* **2009**, *19*, 1093–1099.
13. Beek, W. J. E.; Wienk, M. M.; Janssen, R. A. J. *Adv. Mater.* **2004**, *16*, 1009–1013.
14. He, J. A.; Mosurkal, R.; Samuelson, L. A.; Li, L.; Kumar, J. *Langmuir* **2003**, *19*, 2169–2174.
15. Wu, J. H.; Li, Q. H.; Fan, L. Q.; Lan, Z.; Li, P. J.; Lin, J. M.; Hao, S. C. *J. Power Sources* **2008**, *181*, 172–176.
16. Yang, C.; Yang, Z. M.; Gu, H. W.; Chang, C. K.; Gao, P.; Xu, B. *Chem. Mater.* **2008**, *20*, 7514–7520.
17. Subbaiyan, N. K.; Wijesinghe, C. A.; D'Souza, F. J. *Am. Chem. Soc.* **2009**, *131*, 14646–14647.
18. Wang, P.; Zakeeruddin, S. M.; Comte, P.; Charvet, R.; Humphry-Baker, R.; Grätzel, M. E. *J. Phys. Chem. B* **2003**, *107*, 14336–14341.
19. Gouterman, M. *J. Mol. Spectrosc.* **1961**, *6*, 138–163.
20. Frisch, M.J.; Trucks, G.W.; Schlegel, H.B.; Scuseria, G.E.; Robb, M.A.; Cheeseman, J.R.; Scalmani, G.; Barone, V.; Mennucci, B.; Petersson, G.A. et al., GAUSSIAN 09, Revision A.02, Gaussian, Inc. Wallingford, CT, USA, 2009.
21. Ma, R. M.; Guo, P.; Cui, H. J.; Zhang, X. X.; Nazeeruddin, M. K.; Grätzel, M. J. *Phys. Chem. A* **2009**, *113*, 10119–10124.
22. Hsieh, C. P.; Lu, H. P.; Chiu, C. L.; Lee, C. W.; Chuang, S. H.; Mai, C. L.; Yen, W. N.; Hsu, S. J. E.; Diau, W. G.; Yeh, C. Y. *J. Mater. Chem.* **2010**, *20*, 1127–1134.